Hierarchical Multiobjective Optimization for Independent System Operators (ISOs) in Electricity Markets

Henry Louie, *Student Member, IEEE*, and Kai Strunz

***Abstract*—The creation of competitive electricity markets has increased the complexity of the economics of system operation. Independent system operators (ISOs) perform optimizations based on a market-driven objective function. However, there may be other objectives that the ISO wishes to consider. These objectives are called secondary objectives, as they are dominated by the economic objective. In this paper, a hierarchical multiobjective (HMO) optimization is developed that, through coordinated control of network devices such as phase shifting transformers and series flexible ac transmission systems (FACTS), allows the market objective to be optimized in a global sense, while the secondary objectives are locally optimized. The method is applied to a modified IEEE 30-bus system incorporating a wide-area impact index-minimizing secondary objective. Formulated in this paper, the wide-area impact index accurately measures the effects of parallel flow over multiple lines in a region. Comparisons are made between the HMO's performance with other single and multiple objective optimizations and between the wide-area impact index and traditional parallel flow calculations.**

***Index Terms*—Flexible ac transmission systems (FACTS), multiobjective optimization methods, parallel flows, phase shifters, power system economics, power system optimization.**

I. Introduction

THE Pennsylvania Jersey Maryland (PJM) Interconnection, with historically large west-to-east power flows, is often disturbed by parallel flow from other independent system operators (ISOs) around Lake Erie [1]. This parallel flow may overload tie-lines or lines within the PJM territory. As a consequence, PJM may be forced to curtail some of its inter- and intra-area transactions or redispatch the generation in its area. Unfortunately, parallel flow is a problem that is not only confined to PJM. Other regions such as the Western Electric Coordinating Council (WECC) and the New York ISO have experienced significant problems with parallel flow [1].

It is possible to reduce the amount of parallel flow in an interconnected system if each ISO in that system limits the parallel flow it causes. Network control devices (NCDs) such as phase shifting transformers and series flexible ac transmission system devices (FACTS) [2] can be operated to prevent parallel flow [3], [4]. While reducing parallel flow is beneficial to the neighbors of an ISO, it is not always in the best economic interest of those involved in the ISO's market to do so. Using an NCD to reduce parallel flow may nullify the economic advantages it brings by reducing congestion. The result is an operating point that may not be economically optimal.

It is common for ISOs to employ optimizations to clear their markets based on reliability constraints, bids, and offers for energy submitted by the market participants [5], [6]. The market participants include generation companies, load serving entities, and brokers. The ISO implements the market-clearing optimization results by dispatching the generators and adjusting the NCD settings. This operating point supersedes the operating point for minimal parallel flow.

The reduction of parallel flow is one of several possible secondary operational objectives that an ISO may wish to consider. It is a secondary objective because its optimal operating point is dominated by the market-optimal operating point. Although dominated, it is possible to include a secondary objective in optimization with meaningful results. The inclusion of a secondary objective transforms the market optimization into a multiobjective optimization. However, standard multiobjective optimization techniques may not produce acceptable results. This is because standard multiobjective optimization methods require tradeoffs between the objective functions—an acerbic proposition to an ISO's market participants [7], [8].

In this paper, a hierarchical multiobjective optimization (HMO) technique is developed that allows the ISO to operate the system based on the market-clearing schedule and consider secondary objectives. This is accomplished by constraining the secondary objectives to operate in the optimal solution space of the economic objective. The secondary objective will be optimized in a meaningful manner if its value varies within this solution space. Though there are several possible choices of secondary objectives, this paper develops and uses a novel wide-area impact objective. This objective is related to parallel flow and can be applied to an ISO in an interconnected system wishing to minimize the impact of its operation on another part of the system. The advantages of the HMO method are that the optimal economic operating point is preserved, the program is computationally simple, the method is transparent to the ISO market participants, and it can be implemented with existing market and energy management system (EMS) software.

An overview of the state of the art of multiobjective programming techniques in power system applications is given in Section II. An HMO for economic operation with a wide-area impact secondary objective is formulated in Section III. This HMO is applied to the IEEE 30-bus system to demonstrate the advantages of the multilevel method over existing single and

Manuscript received July 12, 2005; revised August 31, 2005. Paper no. TPWRS-00418-2005.

The authors are with the University of Washington, Seattle, WA 98195-2500 USA.

Digital Object Identifier 10.1109/TPWRS.2006.881151

multiple objective optimizations in Section IV, followed by conclusions in Section V.

II. State of the Art

In electricity markets, single objective optimization is often used to determine the optimal security-constrained system operating point [6]. The independent variables in this problem may include generation values and settings of network devices. The domain of these variables is called the feasible region or solution space. This optimization can be generically expressed as

$$\min f(\boldsymbol{x}) \tag{1}$$

subject to

$$\boldsymbol{x} \in X$$
$$X = (\boldsymbol{x} \in \mathbb{R}^n : \boldsymbol{g}(\boldsymbol{x}) = 0, \boldsymbol{h}(\boldsymbol{x}) \leq 0)$$

where $\boldsymbol{x}$ is an n-dimensional vector of the independent variables, and $\boldsymbol{g}(\boldsymbol{x})$ and $\boldsymbol{h}(\boldsymbol{x})$ are the system equality and inequality constraints, respectively. The set X is the feasible region. A solution $\boldsymbol{x}^*$ to (1) is a global minimum if $f(\boldsymbol{x}) \geq f(\boldsymbol{x}^*)$ for all other $\boldsymbol{x}$. Let the set of all points with $f(\boldsymbol{x}) = f(\boldsymbol{x}^*)$ be called the optimal solution space. If the optimal solution space is a unique point, then $\boldsymbol{x}^*$ is known as the strict global minimum. There is a multitude of optimization methods for solving (1). The selection of a proper method and existence of a strict global minimum is dependent on the nature of the objective and the constraints. It is assumed in this paper that a global minimum can always be found.

Multiobjective optimization problems (MOPs) arise when the objective in (1) is an m-dimensional objective function vector. MOPs occur in power systems primarily in the realm of economic dispatch with environmental considerations [9]. Other applications include active and reactive power dispatching [10] and generator maintenance scheduling in electricity markets [11]. These problems are often solved by obtaining a set of solutions known as a Pareto front. All points in this set have the property of Pareto-optimality [8]. A point $\boldsymbol{x}$ is considered to be Pareto optimal if there is no other point $\bar{\boldsymbol{x}}$ with the property

$$f_i(\bar{\boldsymbol{x}}) \leq f_i(\boldsymbol{x}), \quad \forall i \in (1, 2, \ldots, m) \tag{2}$$

where one of the inequalities is strict. The Pareto front itself provides valuable objective function tradeoff information. A single point is chosen from the Pareto front based on this information.

Several MOP solution methods have been applied to power system problems. A weighted-sum approach to this problem is reported in [12] and a single-level reduced feasible region method in [13]. The weighted-sum method transforms the MOP to a single objective problem by forming different weighted, linear combinations of the objectives. The drawbacks of this method are that multiple optimizations are required, and the set of points generated is not guaranteed to span the entire Pareto-optimal space. Single-level reduced feasible region methods attempt to bind the optimal solution by transforming all but one of the objectives into inequality constraints. This method is generally iterative and may require several optimizations to determine the best solution.

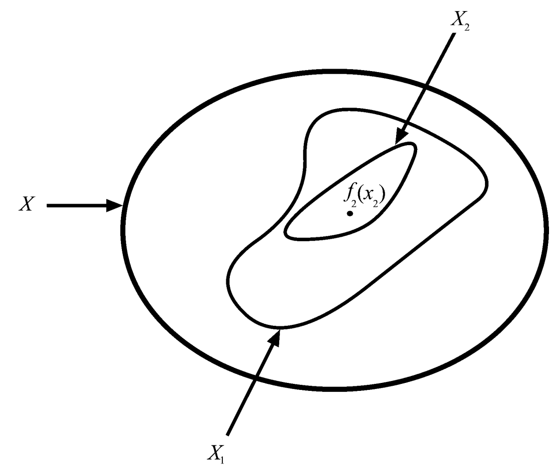

Fig. 1. Conceptual illustration of HMO method.

Specialized methods using evolutionary and stochastic algorithms to obtain the Pareto front have been developed and applied to power system problems [14], [15]. These methods have been shown to adequately find Pareto fronts and do not require several optimization runs. However, if a hierarchical structure exists among the objectives, a Pareto front is not needed because tradeoff information is not required.

III. HMO for Power Systems

A multiobjective problem is hierarchical if the objectives can be ordered by strict preference, where f_1 is the most preferred [16]. The solution $\boldsymbol{x}^*$ to this problem will have the following properties: it is Pareto-optimal, $f_1(\boldsymbol{x}^*)$ is equal to its global minimum, and any point $\boldsymbol{x}$ satisfying $f_k(\boldsymbol{x}) < f_k(\boldsymbol{x}^*)$ will also have the property $f_j(\boldsymbol{x}) > f_j(\boldsymbol{x}^*)$ for at least one j, where $j < k$. In other words, all objectives are minimized in a manner such that they do not cause an increase in any of the more preferred objectives. These problems do not require a multiple point Pareto front, as only one Pareto-optimal point is required and no tradeoff information is needed.

An HMO efficiently solves problems with a hierarchical structure by using a multilevel reduced feasible region method. This procedure is illustrated in Fig. 1. The space X is the entire set of values of $\boldsymbol{x}$. The algorithm begins at the first level by minimizing $f_1(\boldsymbol{x})$ over the feasible region, X_1, as determined by the system constraints. The value of the objective at the optimal point, $\boldsymbol{x}_1$, is used as a constraint for the next level's optimization. A new, reduced feasible set X_2 is created by

$$X_2 = (X_1 : \boldsymbol{x} \in X, f_1(\boldsymbol{x}) = f_1(\boldsymbol{x}_1)). \tag{3}$$

At level 2, the objective $f_2(\boldsymbol{x})$ is minimized over X_2. The solution, $\boldsymbol{x}_2$, corresponding to an objective value of $f_2(\boldsymbol{x}_2)$ is found within X_2. This value is then treated as an additional constraint, further reducing the feasible space. The process continues, reducing the solution space and optimizing a new objective at each level until all objectives have been considered or the solution space becomes unique. The resulting solution, $\boldsymbol{x}_n$, is Pareto-optimal. In general, the spaces created have the relationship

$$\boldsymbol{x}_n \in X_n \subset X_{n-1} \subset \ldots \subset X. \tag{4}$$

The usefulness of this algorithm relies on the non-uniqueness of the optimal solution. If strict global optimality is reached at some level, the feasible region becomes a point for all lower levels, and the optimization ceases [16]. If the upper level objective function is not convex, and a local optimum is found, then this locally optimal value is passed as a constraint to the lower levels. The lower levels will continue to perform their optimizations as described.

It is important to understand that since the solution to the upper level is treated as a constraint on the lower level, the optimal solution of the upper level is effectively insulated from all characteristics of the lower level. This includes the selection of the lower level objective and the solution associated with its minimum.

In this paper, it is assumed that the ISO must operate in accordance with the market-clearing dispatch schedule. As a consequence, a market-dominant, hierarchical objective structure is created. This makes a two-level HMO a natural candidate for market-based multiobjective power system optimization. The upper level clears the market, while the lower level considers a secondary objective.

A. Objectives

1) Market: Electricity markets are typically cleared by running an optimization with the objective of satisfying demand from the cheapest generating source or maximizing social welfare [6]. The cost of energy from each generator is determined by its offer price, not its operating cost. Under inelastic demand conditions, the former objective is used, while price-sensitive demand conditions require the latter. The HMO optimizes the market objective in its upper level. Lower-level optimizations are forced to operate within the optimal space of the upper level, so care must be taken in choosing appropriate secondary objectives.

2) Wide-Area Impact: While it is theoretically possible to consider any objective in the lower level, the HMO has been specifically implemented for line flow objectives. Line flows are sensitive to NCD settings, which can be altered in the lower level. Other objectives such as emission reduction are overly dependent on generation schedules. The lower-level optimization would not be able to significantly affect their value.

Line flow control has applications in parallel flow minimization. Problems caused by parallel flow are manifested in reduced capacity of the impacted area's lines [1]. Parallel flow is measured as the amount of unscheduled power flowing between sources and sinks in one system through tie-lines into other systems [1]. This metric is not always a strong indicator of the effects of parallel flow into that system. The system shown

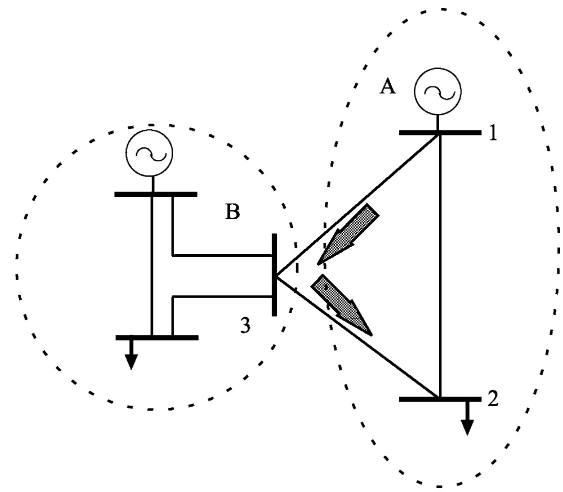

Fig. 2. Two-area system with no impact and large parallel flow.

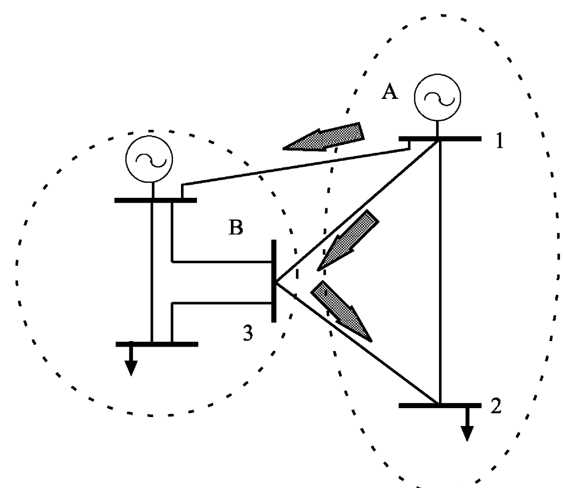

Fig. 3. Two-area system with large impact and large parallel flow.

in Fig. 2 is used to intuitively illustrate this concept. A portion of the power generated in ISO A flows through the tie-lines into and out of ISO B on route to the load at bus 2. The parallel flow is large, but the impact of this operation is minimal as ISO B retains full use of its transmission capacity.

Contrast this example with the system shown in Fig. 3. In this scenario, a line has been between ISOs A and B. The reduction of capacity of ISO B's lines is now a concern, as power flows on the lines inside its region. Again, the amount of parallel flow is not an accurate measure of this reduction in capacity, as much of the power flows into and out of bus 3. This example is representative of a real-world problem: large-capacity wind farms in northern Germany intermittently send power through Belgium on route to loads throughout Germany. Reduced capacity in the lines in Belgium ensues.

It is clear that in some scenarios, the traditional definition of parallel flow has its shortcomings. In order to accurately assess the reduction of line capacity caused by parallel flow, a wide-area impact index is proposed. The index is calculated by the weighted squared norm of the reduction in line capacity of each line due to the parallel flow. This gives ISO A an indication of the effects that its operation has on ISO B. The weighting element is introduced by multiplying an l-dimensional vector of line flows by the diagonal weighting matrix $\boldsymbol{W}$, defined as

$$\boldsymbol{W} = \begin{bmatrix} \alpha_1 & & \mathbf{0} \\ & \ddots & \\ \mathbf{0} & & \alpha_l \end{bmatrix} \tag{5}$$

where α_k is the weight of line k. The weighting allows ISO B to rate each line in its area by system criticality. The weighting factor is applied as follows: for most lines, a nominal value of $\alpha = 1$ is applied, tie or lightly loaded lines are given a low or zero weighting, and critical lines are given higher values such as $\alpha = 3$. Critical lines are lines that are heavily loaded, sensitive for voltage or stability reasons, or whose capacity is important for transactions. Tie-lines containing the NCDs used in the optimization are given weights of zero, as it is the intent of these devices to alter the power flow through them. The specifics of the index calculation depend upon the model formulation used, which are presented in the next section.

B. Mathematical Formulation

1) Linear Formulation: The HMO uses a linear system model with standard dc power flow assumptions [17] and constraints on all of its levels. This ensures a consistency in solution feasibility and minimizes the required input data. Furthermore, the assumptions allow the problem to be formulated without complete real-time data from adjacent ISOs. Through superposition, the formulation is independent from the operating point of other ISOs. NCDs are vital to the size of the lower-level solution spaces. This warrants special attention in their inclusion in optimizations.

Network control devices can be represented by their so-called power injection models [3], [18]–[20]. This model translates the NCD characteristics into power injections at the device terminal buses. Modeled as ideal components with no power loss, the injections are equal in magnitude and opposite in direction. In the linear dc system model, series-connected devices that affect real power, such as thyristor controlled series compensators (TCSC) and phase shifting transformers (PST), are considered.

An optimization with n buses, m generators, r NCDs, and a generic objective function is formulated as

$$\min \{f(\boldsymbol{x})\} \tag{6}$$

subject to

$$\sum_{k=1}^{m} P_{\mathrm{G},k} - \sum_{k=1}^{n} D_k = 0 \tag{7}$$

$$\boldsymbol{P}_{\mathrm{G}}^{\min} \le \boldsymbol{P}_{\mathrm{G}} \le \boldsymbol{P}_{\mathrm{G}}^{\max} \tag{8}$$

$$\boldsymbol{P}_{\mathrm{I}}^{\min} \le \boldsymbol{P}_{\mathrm{I}} \le \boldsymbol{P}_{\mathrm{I}}^{\max} \tag{9}$$

$$\boldsymbol{H\theta} \le \boldsymbol{F}^{\max} \tag{10}$$

$$-\boldsymbol{H\theta} \le \boldsymbol{F}^{\max} \tag{11}$$

where $\boldsymbol{x}$ is a vector of the independent variables, $\boldsymbol{P}_{\mathrm{G}}$ is an m-dimensional vector of committed generator real power injections, $\boldsymbol{D}$ is an n-dimensional vector of loads at each bus, $\boldsymbol{P}_{\mathrm{I}}$ is an r-dimensional vector of equivalent power injections of NCD, and $\boldsymbol{\theta}$ is a vector of bus angles [6], [21]. This angle vector is a linear function of generation, load, as well as NCD equivalent power injections and withdrawals at each bus. Finally, $\boldsymbol{H}$ is a matrix of branch flow thermal and/or stability constraint coefficients whose values are determined by the bus impedance matrix and the location of the NCD devices [21]. In this formulation, the variables are considered continuous in nature. Power generation and device injection limits are represented in (8) and (9), respectively. It is important to note that in the case of TCSCs, the power injection limits cannot be explicitly stated; however, they can be expressed linearly in terms of the other injections [21]. The line flow constraints for each direction are represented in (10) and (11). The objective in (6) is defined at each level of the HMO. The upper level is always economics based, while the lower level is left to user discretion.

Of interest are the conditions in which the upper-level optimal solution is not a strict minimum. At the completion of the upper-level optimization, the optimal generation schedule and NCD settings are determined. Most likely, the solution with respect to the generator values is unique, but there might be a range of values that the NCDs can attain without straying from the optimal objective function value. If this is the case, the solution is not a strict minimum, and the lower-level optimization will not be confined to a point but will operate within a space of NCD values. This space is represented as X_2 in Fig. 1. The existence of this condition can be determined by perturbing the NCD values around the optimal solution and checking to see if the Kuhn–Tucker conditions are still upheld. The Kuhn–Tucker conditions for (6) are

$$\begin{aligned}\nabla f(\boldsymbol{x}) &+ \nabla\lambda\left(\sum_{k=1}^{m} P_{\mathrm{G},k} - \sum_{k=1}^{n} D_k\right) + \nabla\boldsymbol{\mu}^{\mathrm{T}}\left(\boldsymbol{P}_{\mathrm{G}} - \boldsymbol{P}_{\mathrm{G}}^{\max}\right)\\ &+\nabla\boldsymbol{\pi}^{\mathrm{T}}\left(\boldsymbol{P}_{\mathrm{G}}^{\min} - \boldsymbol{P}_{\mathrm{G}}\right) + \nabla\boldsymbol{\tau}^{\mathrm{T}}\left(\boldsymbol{P}_{\mathrm{I}}^{\min} - \boldsymbol{P}_{\mathrm{I}}\right)\\ &+\nabla\boldsymbol{\eta}^{\mathrm{T}}\left(\boldsymbol{P}_{\mathrm{I}} - \boldsymbol{P}_{\mathrm{I}}^{\max}\right)\\ &+\nabla\boldsymbol{\rho}^{\mathrm{T}}(-\boldsymbol{H\theta} - \boldsymbol{F}^{\max}) + \nabla\boldsymbol{\gamma}^{\mathrm{T}}\left(\boldsymbol{H\theta} - \boldsymbol{F}^{\max}\right) = \mathbf{0}\end{aligned} \tag{12}$$

$$\boldsymbol{\mu}^{\mathrm{T}}\left(\boldsymbol{P}_{\mathrm{G}} - \boldsymbol{P}_{\mathrm{G}}^{\max}\right) = 0 \tag{13}$$

$$\boldsymbol{\pi}^{\mathrm{T}}\left(\boldsymbol{P}_{\mathrm{G}}^{\min} - \boldsymbol{P}_{\mathrm{G}}\right) = 0 \tag{14}$$

$$\boldsymbol{\eta}^{\mathrm{T}}\left(\boldsymbol{P}_{\mathrm{I}} - \boldsymbol{P}_{\mathrm{I}}^{\max}\right) = 0 \tag{15}$$

$$\boldsymbol{\tau}^{\mathrm{T}}\left(\boldsymbol{P}_{\mathrm{I}}^{\min} - \boldsymbol{P}_{\mathrm{I}}\right) = 0 \tag{16}$$

$$\boldsymbol{\gamma}^{\mathrm{T}}(\boldsymbol{H\theta} - \boldsymbol{F}^{\max}) = 0 \tag{17}$$

$$\boldsymbol{\rho}^{\mathrm{T}}(-\boldsymbol{H\theta} - \boldsymbol{F}^{\max}) = 0 \tag{18}$$

$$\boldsymbol{\mu}, \boldsymbol{\pi}, \boldsymbol{\eta}, \boldsymbol{\tau}, \boldsymbol{\gamma}, \boldsymbol{\rho} \ge \mathbf{0} \tag{19}$$

where $\boldsymbol{P}_{\mathrm{G}}$ and $\boldsymbol{P}_{\mathrm{I}}$ are the optimal generation and device values determined by the upper level, respectively; λ is the scalar Lagrange multiplier associated with the power balance equation; and $\boldsymbol{\mu}$, $\boldsymbol{\pi}$, $\boldsymbol{\eta}$, $\boldsymbol{\tau}$, $\boldsymbol{\gamma}$, and $\boldsymbol{\rho}$ are vectors of Lagrange multipliers associated with generator maximum and minimum, NCD injection maximum, and minimum and directional line flow limits, respectively [22]. The gradient is taken with respect to the generator and NCD injections and the Lagrange multipliers.

For illustrative purposes, consider a simple system with one NCD. The optimal solution is not unique if $P_{\rm I}$ can be perturbed to a feasible value, $\bar{P}_{\rm I}$, without violating (12)–(19). The complementary slackness conditions (13)–(18) hold for any $\bar{P}_{\rm I}$ if $\boldsymbol{\eta}$, $\boldsymbol{\tau}$, $\boldsymbol{\gamma}$, and $\boldsymbol{\rho}$ are zero. This is a necessary condition for non-uniqueness that occurs when $\bar{P}_{\rm I}$ and the line flows are strictly within their respective limits. In addition, since (6) is not a function of $P_{\rm I}$, then (12) is equal to zero, regardless of $\bar{P}_{\rm I}$. Therefore, under these conditions, $P_{\rm I}$ can be perturbed without violating the Kuhn–Tucker optimality conditions, and the solution to the upper-level optimization will not be unique. This analysis can be extended to a number of NCDs without loss of meaning.

Solutions to problems formulated as in (6)–(11) with no strict global minimum have a tendency to place otherwise unbinding inequality constraints at their limits [22]. This makes it unlikely, though not impossible, for a single objective optimization to yield the same result as the HMO.

2) Nonlinear Formulation: The formulations in this paper are based on standard dc power flow assumptions and inherently ignore resistance. Though most ISOs do not use a nonlinear ac model in all of their market calculations [5], discussion here is warranted. If such a model is used, alterations to the algorithm are needed to provide meaningful results. The operation of the network control devices to alter power flow will inherently cause system losses to change. This in turn will change the amount of generation needed. The added amount, although often negligible, will likely result in a unique optimal solution in the upper level, rendering the lower-level optimization ineffective. Allowing for a small amount of extra cost to cover additional losses can be achieved by expanding the upper-level optimal solution space to be

$$X_2 = (X : \boldsymbol{x} \in X, f(\boldsymbol{x}) \leq f(\boldsymbol{x}_1) + \delta) \tag{20}$$

where δ is positive and is the predetermined cost of extra generation the ISO is willing to allow to make up for any additional losses.

3) Upper-Level Optimization: Many ISOs clear their markets based on the offers received by generating companies. These curves can be linear, piecewise linear, or quadratic, among other possibilities. For illustrative purposes, in this paper, the offer curves are assumed to be quadratic, though the method itself can be applied to any curve type. The ISO clears the market based on the following objective:

$$f = \frac{1}{2}\boldsymbol{P}_{\rm G}^{\rm T}\boldsymbol{Q}\boldsymbol{P}_{\rm G} + \boldsymbol{d}^{\rm T}\boldsymbol{P}_{\rm G} \tag{21}$$

where $\boldsymbol{Q}$ is a diagonal matrix of quadratic generator offer function coefficients, and $\boldsymbol{d}$ is a vector of linear generator offer function coefficients [6]. This objective is independent of all $P_{\rm I}$, allowing the possibility of non-unique solutions.

4) Lower-Level Optimization: In accordance with the linear problem formulation, the total real power flowing on any line under standard dc power flow assumptions is found by

$$\boldsymbol{F} = \boldsymbol{H}\boldsymbol{\theta} \tag{22}$$

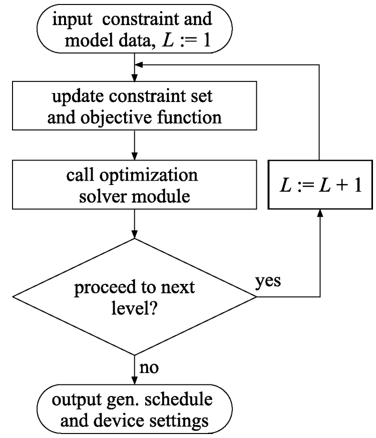

Fig. 4. Flowchart of HMO implementation.

where $\boldsymbol{F}$ is a vector of line flows. As previously mentioned, $\boldsymbol{\theta}$ is a linear function of net power injections. Since the system is linear, it is possible to calculate the amount that a particular bus's net power injection contributes to any line flow. If the bus injections are limited to those within ISO A, and $\boldsymbol{F}$ only contains lines inside or into ISO B, then (22) gives the power flow on the lines in ISO B as a result of ISO A's operation. This allows (22) to be rewritten as

$$\boldsymbol{F} = \boldsymbol{\Psi}\boldsymbol{P}_{\rm net} \tag{23}$$

where $\boldsymbol{P}_{\rm net}$ is a vector of net power injections at each bus. This is the sum of $P_{\rm G}$ and $P_{\rm I}$ minus the load at each bus. The matrix $\boldsymbol{\Psi}$ is a concatenation of injection shift factors arranged as

$$\begin{bmatrix} F_{ij} \\ \vdots \\ F_{kl} \end{bmatrix} = \begin{bmatrix} \psi_{ij,1} & \cdots & \psi_{ij,n} \\ \vdots & & \vdots \\ \psi_{kl,1} & \cdots & \psi_{kl,n} \end{bmatrix} \begin{bmatrix} P_{\rm net1} \\ \vdots \\ P_{{\rm net}n} \end{bmatrix} \tag{24}$$

where $\psi_{ij,k}$ is the injection shift factor from a bus k onto a line $i-j$, and F_{ij} is the real power flow on line $i-j$ computed as

$$\psi_{ij,k} = \frac{z_{jk} - z_{ik}}{\bar{x}_{ij}} \tag{25}$$

where $\bar{x}_{ij}$ is the simple reactance of line $i-j$, and z_{ik} are the elements of the bus impedance matrix under standard dc power flow assumptions [23].

The linearity of the system allows this formulation to be independent of the actual operating conditions of ISO B. The wide-area impact index objective function is defined as

$$f = ||\boldsymbol{W}\boldsymbol{\Psi}\boldsymbol{P}_{\rm net}||^2 \tag{26}$$

where $\boldsymbol{W}$ is the weighting matrix defined in (5), and f is the resulting impact index. The lower-level optimization minimizes (26) using quadratic programming within the feasible region created by (7)–(11) and the optimal solution to (21).

C. Implementation

The implementation of the HMO, like other proposed network element-based market concepts [24], can be accommodated into most electricity markets. A flowchart for a two-level

HMO applied to a linear dc system model is given in Fig. 4. The program begins by loading data: injection shift factor data for ISO B, generation offers, system constraints, generator and NCD limits, and system topological information for both ISOs. The level counter L is set to 1. Based on the loaded data, the program sets the constraints, converts the NCD into power injections, and loads the upper-level objective. This information is passed into the optimization solver module. The solver performs the optimization; the single objective optimization method used is dependent on the type of objective function and constraints. Once solved, the program performs a termination check. The program should proceed to the output module if the solution to the upper level is unique, or if $L = 2$. Solution uniqueness is determined by checking the Lagrange multipliers. Uniqueness is concluded if all Lagrange multipliers have nonzero values. If neither of the termination conditions are satisfied, L is increased, and the current solution is passed as a constraint to the next program iteration. Upon main loop termination, the output module converts the equivalent power injections into NCD settings. These controller settings are exported along with the generation schedule.

An important feature of the HMO is that it can be integrated into existing EMS and market-clearing optimization software. The extra inputs needed are the injection shift factors and line weighting data of the adjacent ISOs. This information requires little memory and only needs to be updated when a line weighting or topology change has occurred. Furthermore, if both objectives are based on the same linear or nonlinear model, the independent variables and system limits can be reused at each level. The upper-level optimization is exactly the same as in the ISO's existing software. If a lower level's objective function is incommensurable with the upper level's optimization technique, a different method can be employed. This is an attractive feature, as it allows the most efficient optimization algorithm to be employed at each level.

The algorithm is altered when the ISO is interconnected with several other ISOs in a large system. If there is a strict priority order among the connected ISOs as far as parallel flow is concerned, a lower level is added for each additional ISO. If there is no clear order, each ISO submits their weightings. In order to ensure relative uniformity among the submissions, the weightings are normalized so that the average value in each area is equal to one. The HMO then proceeds as described previously with only one lower level.

IV. Validation and Application

A modified version of the IEEE 30-bus system is used to demonstrate the proposed two-level HMO. Special attention is given to the progression of solution space at each level. The solution is compared to two single objective optimizations, the objectives of which correspond to either the upper- or lower-level HMO objectives and to the results of a nonlinear HMO. The method is then compared to a weighted-sum technique, where its superiority in handling hierarchical problems over those requiring a Pareto front is shown. The weighted-sum method is selected for comparison, as its integration into existing software is similar to that of the HMO in that its main requirement is a change in objective functions. This differs from other MOP methods, such as those that employ evolutionary or stochastic algorithms, as they require a new optimization procedure. The effectiveness of the wide-area impact optimization is shown by a comparison with a parallel flow minimizing optimization.

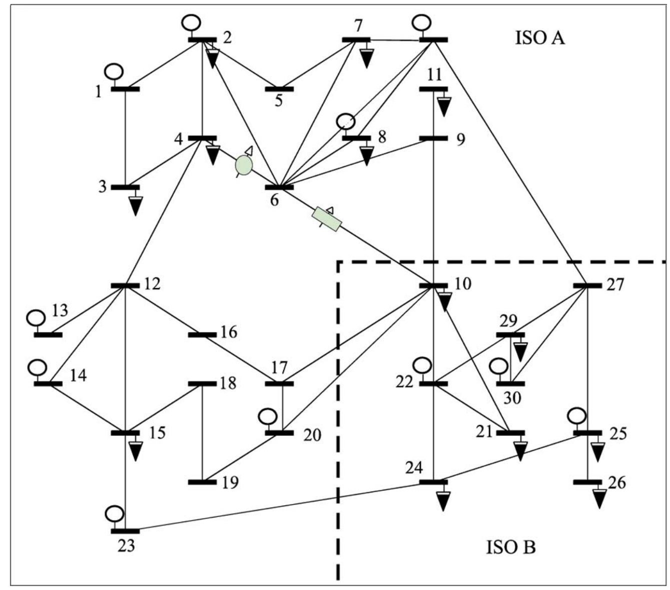

Fig. 5. Modified IEEE 30-bus system.

TABLE I
NETWORK CONTROL DEVICE PARAMETERS

Type	Injection Bus	Withdrawal Bus	Min Setting	Max Setting
PST	4	6	−20.0°	15.0°
TCSC	6	10	−20.0 %	0.0 %

A. System Specifications

The system, shown in Fig. 5, is partitioned into two tightly meshed regions, each operated by a different ISO. There are no transactions from ISO A to ISO B. The upper- and lower-level objectives of ISO A are to minimize the cost of generation and reduce the wide-area impact index, respectively. Generation offers are quadratic, and the demand is inelastic. The system is populated with two different NCDs to illustrate the HMO's ability to coordinate and integrate different device types. A PST and a TCSC are controlled by ISO A with parameters given in Table I. The TCSC range is given in percent of line impedance. A binding thermal limit of 50 MW is imposed on line 2–4, and the maximum output of each generator is 500 MW. Additional lines have been added to the system to emphasize the wide-area impact index. The line flow weights are shown in Table II. The nominal value for a line within ISO B is unity. Tie-lines are given a weight of 0.125, with the exception of the line containing the TCSC, which is weighted at zero. For illustrative purposes, line 25–27 is weighted as 2. The load and generation of ISO A have been adjusted so that the potential for large parallel flow

TABLE II
ISO B LINE FLOW

To Bus No.	From Bus No.	α Weight Factor	Parallel Obj. Line Flow (MW)	Imp. Obj. I Line Flow (MW)	Imp. Obj. II Line Flow (MW)
6	10	0.000	27.44	30.80	34.19
9	10	0.125	−36.78	−44.92	−43.38
10	20	0.125	0.00	−1.89	−0.56
10	17	0.125	−2.64	−6.98	−3.96
23	24	0.125	−4.18	−1.43	−3.04
28	27	0.125	10.87	6.68	7.71
10	21	1.000	−4.04	−3.17	−2.82
10	22	1.000	−2.65	−2.08	−1.85
21	22	1.000	−4.04	−3.17	−2.81
22	24	1.000	−0.14	−1.03	−0.04
24	25	1.000	−4.32	−2.46	−3.07
25	26	1.000	0.00	0.00	0.00
25	27	2.000	−4.32	−2.46	−3.07
27	29	1.000	4.70	3.03	3.33
27	30	1.000	1.85	1.19	1.31
29	22	1.000	6.55	4.22	4.63
29	30	1.000	−1.85	−1.19	−1.31
Total Parallel Flow (MW)			81.91	92.70	92.84
Impact Index			228.14	118.74	105.02
Total Flow In ISO B (MW)			34.46	24.01	24.25

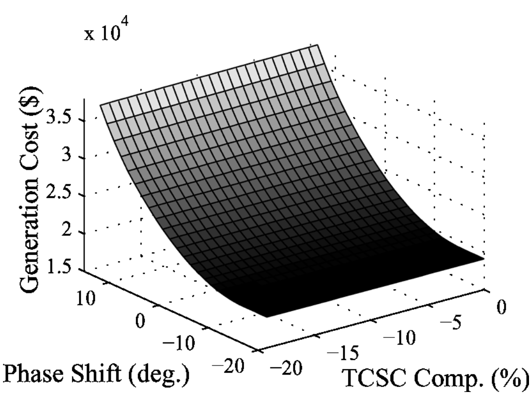

Fig. 6. Upper-level solution space.

exists. The new load and optimal generation values for each objective are found in the Appendix.

B. Solution Space

The imposition of line limits constricts the upper-level solution space. Fig. 6 shows the upper-level solution space with minimized generation cost with respect to the NCD settings. The surface plateaus at a minimum value for TCSC compensations between -20 and 0% and for phase shift angles between $-15.4°$ and its limit, $-20°$. The solution to the upper-level optimization is therefore not unique.

The impact index values corresponding to the NCD settings inside the optimal solution space of the upper level are shown in Fig. 7. This surface is the solution space of the lower level. From this surface, it is seen that the optimal device settings are a phase shift of $-20°$ and a TCSC compensation of -20%.

C. Optimization Results

The HMO solution is now compared to those obtained by other optimization methods. Table III shows the generation cost and impact index associated with the optimal solutions of the HMO and two single objective optimizations. From this table,

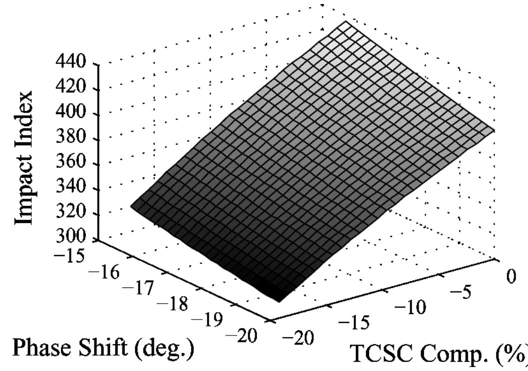

Fig. 7. Lower-level solution space.

TABLE III
OPTIMIZATION RESULTS

Objective	Gen. Cost ($)	Imp. Index	PST (deg)	TCSC (%)
HMO	19,110	307.3	−20.0	−20.0
Market	19,110	357.4	−15.4	−15.8
Impact Index	29,052	118.7	−20.0	−20.0

it is seen that the HMO clears the market with the same results as the market only optimization but with a 14% reduction in impact index. The generation costs are the same because the optimization of the upper level is identical to the single objective optimization. It is important to note that the economic-only optimization has set the TCSC value to -15.8%, though any value within its limit would yield the minimum cost. This reflects the optimization algorithm's tendency to set nonbinding constraints to their limits. In this case, the flow on line 2–4 is unnecessarily set to its limit of 50 MW.

The HMO impact index is greater than the value by the impact index-only optimization. However, this decrease comes at a price, as the cost of generation escalates to over 150% of the minimum cost. The results of this single objective comparison can be summarized as follows: as evidenced by Table III, the HMO observes the strict dominance structure of the objectives and is able to replicate the minimal generation cost in the presently used economics-only optimization, and the nonunique optimal solution of the upper level has given the lower level a meaningful solution space in which to operate, resulting in a decreased impact index.

The effects of the standard dc power flow assumptions are now analyzed against a nonlinear ac optimization and system model. The first row of Table IV shows the HMO solution when a full ac model is used. In this case, δ in (20) is set to be 3% of the minimum cost. The second row shows the results when the solution to the linear HMO is applied to the nonlinear system model. Due to the inclusion of losses, the generation schedule was adjusted to reflect up to a 3% increase in costs. It is seen that both the objectives and device set points are similar and that the standard dc power flow assumptions provide a reasonable approximation.

D. Weighted-Sum Comparison

A competing method of multiobjective optimization is the weighted-sum approach. A 30-point front developed by a

TABLE IV
LINEAR AND NONLINEAR HMO RESULTS

Model	Gen. Cost ($)	Imp. Index	PST (deg)	TCSC (%)
Non-linear	20,546	299.2	−18.7	−20.0
Linear	20,547	311.2	−20.0	−20.0

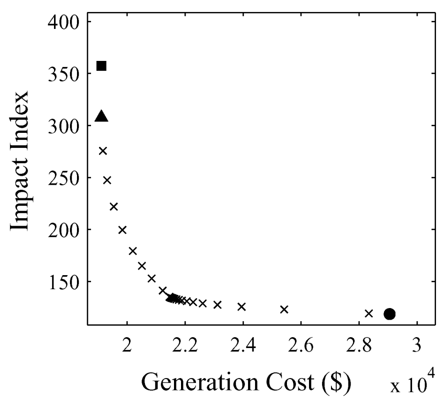

Fig. 8. Objective values generated by weighted-sum method with HMO solution added.

weighted-sum method is given by the cross marks in Fig. 8. The circle and square marks indicate the value when the weighting is zero for the market and impact objectives, respectively. The triangle mark has been added to this front to indicate the location of the HMO solution and was not obtained through the weighted-sum method. Note that these results agree with Table III.

From this figure, two characteristics are observed. First, the weighted-sum method produces a multitude of points, while the HMO generates a single point. These extra points provide information on the tradeoffs involved between the market and impact objectives. However, if the ISO has a strictly hierarchical objective function structure, then this tradeoff information is not needed. Second, the HMO solution is not on the weighted-sum front, even with a zero impact index weighting. While it is possible to interpolate the front to arrive at a point near the HMO solution, this approach is flawed. This interpolated point will have a generation cost that is greater than the HMO's solution, and solving the inverse problem of obtaining the generation schedule and device settings from the interpolated point requires yet another optimization.

In general, unless the upper-level solution is unique, the solution to the HMO cannot be found by a weighted-sum method; an evolutionary or stochastic search algorithm is needed to find the point. This indicates that a weighted-sum approach cannot be applied universally to hierarchical problems. Therefore, the use of HMO for solving multiobjective power system optimization problems in a market environment is warranted.

E. Wide-Area Impact Index Validation

The results of the single objective impact index optimization provide additional insight into the wide-area impact index. Table II shows the line flows in ISO B for two optimizations. The flows in the fourth column are obtained from the impact index optimization, and the fifth column is from a magnitude of parallel flow minimizing optimization. Tie-line flows are given in the first six rows. As there are no scheduled transactions, all power flowing on the tie-lines can be considered parallel flow.

The parallel flow of the parallel flow minimizing optimization is over 10% lower than the impact index minimization, from 92.7 to 81.19 MW. However, the impact index of this line flow profile is nearly twice that of the index minimization, as seen in the second to last row of the table. The total MW flowing on ISO B as a result of ISO A's operation for each objective is given in the final row of the table. From this, it is seen that the wide-area impact index minimization is able to decrease this flow by over 30%, from 34.46 to 24.01 MW. This amount is the real harm caused by the parallel flow. In addition, the index optimization reduces the flow on the critical line by 40% over the parallel flow optimization. This is due to the higher weighting placed on this line. Alternatively, if line 22–24 is given a weighting of 10, the solution changes with flows shown in the last column of Table II. Note that the flow on this line has been reduced by almost 97%.

This case typifies the shortcomings of traditionally defined parallel flow in tightly meshed systems and the ability of the wide-area impact index to effectively reduce the flow within a large area.

V. CONCLUSION

It has been shown that the HMO is capable of determining generation schedules and device set points for a market-driven objective and reduced wide-area impact. This method requires no knowledge of objective function tradeoffs. Furthermore, unlike other MOP solvers that may require several optimizations to find a Pareto front, the number of optimizations in HMO is always less than or equal to the number of objectives. The HMO solution is Pareto-optimal, and the economics-dominant structure of objective functions is guaranteed. The method can be incorporated into existing ISO software and only periodically requires impedance or injection shift factor data from the affected ISO. This allows the optimization to be run independent of the actual operating point of the adjacent ISOs. These features allow an ISO to make full use of an already installed device, thereby increasing its utility and value.

The proposed wide-area impact index accurately measures the reduction in line capacity caused by the parallel flow, not just the parallel flow amount. The index has been incorporated into an optimization with an injection shift factor-based quadratic objective and linear constraints. This method has been shown to be superior in limiting the total unscheduled flow on lines within a wide area. In addition, the optimization is sensitive to line weighting and is therefore more adaptive than traditional methods.

Further work in this area could focus on multiobjective optimization methods in which the operation of the NCDs is not centrally controlled. In addition, the adaptation of the HMO to different markets, such as those using loss factors or dispatchable transmission, would be beneficial in understanding the breadth of the method's application.

TABLE V
SYSTEM LOAD AND GENERATION DATA

Bus	Load (MW)	Market Obj. Gen. (MW)	Impact Obj. Gen. (MW)	Q Coeff.	d Coeff.
1	-	227.58	500.00	0.1750	5.0
2	80	218.66	90.72	0.1684	8.0
3	150	-	-	-	-
4	120	-	-	-	-
7	40	-	-	-	-
8	200	173.36	139.28	0.2067	9.0
11	90	-	-	-	-
15	50	-	-	-	-
28	-	110.40	0.00	0.3200	9.5

APPENDIX
SYSTEM DATA

The load and optimal generation data for buses within ISO A are given in Table V. The fifth and sixth columns are coefficients of the generator offer functions used in (21). The lines that have been added to the standard system are between buses 7 and 8, 17 and 20, and 29 and 22.

ACKNOWLEDGMENT

The authors would like to thank the Advanced Power Technologies (APT) members for supporting this paper. The APT Center is supported by Areva T&D, Bonneville Power Administration, CESI, LG Industrial Systems, PJM Interconnection, and RTE France.

REFERENCES

[1] D. Hayward *et al.*, "Operating problems with parallel flows," *IEEE Trans. Power Syst.*, vol. 6, no. 3, pp. 1024–1034, Aug. 1991.
[2] N. G. Hingorani and L. Gyugyi, *Understanding FACTS: Concepts and Technology of Flexible AC Transmission Systems*. Piscataway, NJ: IEEE Press, 1999.
[3] D. J. Gotham and G. T. Heydt, "Power flow control and power flow studies for systems with FACTS device," *IEEE Trans. Power Syst.*, vol. 13, no. 1, pp. 60–65, Feb. 1998.
[4] Y. Xiao, Y. H. Song, and Y. Z. Sun, "Power flow control approach to power systems with embedded FACTS devices," *IEEE Trans. Power Syst.*, vol. 17, no. 4, pp. 943–949, Nov. 2002.
[5] A. L. Ott, "Experience with PJM market operation, system design, and implementation," *IEEE Trans. Power Syst.*, vol. 18, no. 2, pp. 582–534, May 2003.
[6] R. D. Christie, B. F. Wollenberg, and I. Wangensteen, "Transmission management in the deregulated environment," *Proc. IEEE*, vol. 88, no. 2, pp. 170–195, Feb. 2000.
[7] R. Steuer, *Multiple Criteria Optimization*. New York: Wiley, 1986.
[8] Y. Sawaragi, H. Nakayama, and T. Tanino, *Theory of Multiobjective Optimization*. Orlando, FL: Academic, 1985.
[9] J. H. Talaq, F. El-Hawary, and M. E. El-Hawary, "A summary of environmental/economic dispatch algorithms," *IEEE Trans. Power Syst.*, vol. 9, no. 3, pp. 1508–1516, Aug. 1994.
[10] B. Serrano and A. Vargas, "Active-reactive power economic dispatch of very short term in competitive electric markets," in *Proc. IEEE Porto Power Tech.*, Sep. 10–13, 2001, vol. 1, pp. 1–6.
[11] W. Peng, M. Rui, X. Tao, Y. Huachun, and H. Renmu, "Research on multi-objective optimum model of unit maintenance scheduling under the condition of electricity market," in *Proc. IEEE Conf. Electric Utility Deregulation, Restructuring, Power Technologies (DRPT)*, Apr. 5–8, 2004, vol. 1, pp. 197–199.
[12] C. S. Chang, K. P. Wong, and B. Fan, "Security-constrained multiobjective generation dispatch using bicriterion global optimization," *Proc. Inst. Elect. Eng., Gen., Transm., Distrib.*, vol. 142, no. 4, pp. 406–414, Jul. 1995.
[13] R. Yokoyama, S. H. Bae, T. Morita, and H. Sasaki, "Multiobjective optimal generation dispatch based on probability security criteria," *IEEE Trans. Power Syst.*, vol. 3, no. 1, pp. 317–324, Feb. 1988.
[14] M. A. Abido, "Environmental/economic power dispatch using multiobjective evolutionary algorithms," *IEEE Trans. Power Syst.*, vol. 18, no. 4, pp. 1529–1537, Nov. 2003.
[15] D. B. Das and C. Patvardhan, "New multi-objective stochastic search technique for economic load dispatch," *Proc. Inst. Elect. Eng., Gen., Transm., Distrib.*, vol. 145, no. 6, pp. 747–752, Nov. 1998.
[16] I. Das, Multi-Objective Optimization. [Online]. Available: http://www-fp.mcs.anl.gov/otc/Guide/OptWeb/multiobj/ (Jan. 1997).
[17] J. Grainger and W. Stevenson, *Power System Analysis*. New York: McGraw-Hill, 1994.
[18] Z. Han, "Phase shifter and power flow control," *IEEE Trans. Power App. Syst.*, vol. PAS-101, no. 10, pp. 3790–3794, Oct. 1982.
[19] G. N. Taranto, L. M. V. G. Pinto, and M. Pereira, "Representation of FACTS devices in power system economic dispatch," *IEEE Trans. Power Syst.*, vol. 7, no. 2, pp. 572–576, May 1992.
[20] M. Noroozian and G. Andersson, "Power flow control by use of controllable series components," *IEEE Trans. Power Del.*, vol. 8, no. 3, pp. 1420–1429, Jul. 1993.
[21] X. Wang, Y. H. Song, Q. Lu, and Y. Z. Sun, "Series FACTS devices in financial transmission rights auction for congestion management," *IEEE Power Eng. Rev.*, vol. 21, no. 11, pp. 41–44, Nov. 2001.
[22] D. Luenberger, *Linear and Nonlinear Programming*. Norwell, MA: Kluwer, 2003.
[23] P. W. Sauer, K. E. Reinhard, and T. J. Overbye, "Extended factors for linear contingency analysis," in *Proc. 34th Hawaii Int. Conf. System Science*, 2001, pp. 697–703.
[24] R. P. O'Neill, R. Baldick, U. Helman, M. H. Rothkopf, and W. Stewart, Jr., "Dispatchable transmission in RTO markets," *IEEE Trans. Power Syst.*, vol. 20, no. 1, pp. 171–179, Feb. 2005.

Henry Louie (S'03) received the B.S.E.E. degree from Kettering University, Flint, MI, in 2002 and the M.S.E.E. degree from the University of Illinois at Urbana-Champaign in 2004. He is presently pursuing the Ph.D. degree at the University of Washington, Seattle.

His research interests include power system optimization and economics.

Kai Strunz received the Dipl.-Ing. degree and the Dr.-Ing. degree (summa cum laude) from the University of Saarland, Saarbrücken, Germany, in 1996 and 2001, respectively.

From 1995 to 1997, he pursued research at Brunel University, London, U.K. From 1997 to 2002, he worked at the Division Recherche et Développement of Electricité de France (EDF), Paris, France. In 2002, he joined the University of Washington, Seattle, as an Assistant Professor. He is the Convener of CIGRE Task Force C6.04.02 on computational tools for the study of distributed energy resources.

Dr. Strunz received the Dr.-Eduard-Martin Award from the University of Saarland in 2002, the National Science Foundation (NSF) CAREER Award in 2003, and the Outstanding Teaching Award from the Department of Electrical Engineering of the University of Washington in 2004.